

Testing for Intrinsic Type Ia Supernova Luminosity Evolution at $z > 2$ with *JWST*

J. D. R. PIEREL,^{1,*} D. A. COULTER,¹ M. R. SIEBERT,¹ H. B. AKINS,² M. ENGESSE,¹ O. D. FOX,¹ M. FRANCO,^{3,2} A. REST,^{1,4}
A. AGRAWAL,⁵ Y. AJAY,⁴ N. ALLEN,^{6,7} C. M. CASEY,^{8,2,6} C. DE COURSEY,⁹ N. E. DRAKOS,¹⁰ E. EGAMI,⁹ A. L. FAISST,¹¹
S. GEZARI,¹ G. GOZALIASL,^{12,13} O. ILBERT,¹⁴ D. O. JONES,¹⁵ M. KARMEN,⁴ J. S. KARTALTEPE,¹⁶ A. M. KOEKEMOER,¹
Z. G. LANE,¹⁷ R. L. LARSON,¹⁶ T. LI,¹⁸ D. LIU,¹⁹ T. J. MORIYA,^{20,21,22} H. J. MCCRACKEN,²³ L. PAQUEREAU,²³ R. M. QUIMBY,^{24,25}
R. M. RICH,²⁶ J. RHODES,²⁷ B. E. ROBERTSON,²⁸ D. B. SANDERS,²⁹ M. SHAHBANDEH,¹ M. SHUNTOV,^{6,7} J. D. SILVERMAN,^{25,30}
L. G. STROLGER,¹ S. TOFT,^{6,7} AND Y. ZENATI^{4,1,†}

¹Space Telescope Science Institute, Baltimore, MD 21218, USA

²The University of Texas at Austin, 2515 Speedway Blvd Stop C1400, Austin, TX 78712, USA

³CEA, Université Paris-Saclay, Université Paris Cité, CNRS, AIM, 91191, Gif-sur-Yvette, France

⁴Physics and Astronomy Department, Johns Hopkins University, Baltimore, MD 21218, USA

⁵Department of Astronomy, University of Illinois at Urbana-Champaign, 1002 W. Green St., IL 61801, USA

⁶Cosmic Dawn Center (DAWN), Denmark

⁷Niels Bohr Institute, University of Copenhagen, Jagtvej 128, DK-2200, Copenhagen, Denmark

⁸Department of Physics, University of California, Santa Barbara, Santa Barbara, CA 93109, USA

⁹Steward Observatory, University of Arizona, 933 N. Cherry Avenue, Tucson, AZ 85721 USA

¹⁰Department of Physics and Astronomy, University of Hawaii, Hilo, 200 W Kawili St, Hilo, HI 96720, USA

¹¹Caltech/IPAC, MS 314-6, 1200 E. California Blvd. Pasadena, CA 91125, USA

¹²Department of Computer Science, Aalto University, P.O. Box 15400, FI-00076 Espoo, Finland

¹³Department of Physics, University of, P.O. Box 64, FI-00014 Helsinki, Finland

¹⁴Aix Marseille Univ, CNRS, CNES, LAM, Marseille, France

¹⁵Institute for Astronomy, University of Hawai'i, 640 N. A'ohoku Pl., Hilo, HI 96720, USA

¹⁶Lab for Multiwavelength Astrophysics, School of Physics and Astronomy, Rochester Institute of Technology, 84 Lomb Memorial Dr., Rochester, NY 14623, USA

¹⁷School of Physical and Chemical Sciences — Te Kura Matū, University of Canterbury, Private Bag 4800, Christchurch 8140, New Zealand

¹⁸Institute of Cosmology and Gravitation, University of Portsmouth, Burnaby Road, Portsmouth, PO1 3FX, UK

¹⁹Purple Mountain Observatory, Chinese Academy of Sciences, 10 Yuanhua Road, Nanjing 210023, China

²⁰National Astronomical Observatory of Japan, National Institutes of Natural Sciences, 2-21-1 Osawa, Mitaka, Tokyo 181-8588, Japan

²¹Graduate Institute for Advanced Studies, SOKENDAI, 2-21-1 Osawa, Mitaka, Tokyo 181-8588, Japan

²²School of Physics and Astronomy, Monash University, Clayton, Victoria 3800, Australia

²³Institut d'Astrophysique de Paris, UMR 7095, CNRS, and Sorbonne Université, 98 bis boulevard Arago, F-75014 Paris, France

²⁴Department of Astronomy/Mount Laguna Observatory, SDSU, 5500 Campanile Drive, San Diego, CA 92812-1221, USA

²⁵Kavli Institute for Physics and Mathematics of the Universe, The U. of Tokyo, Kashiwa, Chiba 277-8583, Japan

²⁶Department of Physics and Astronomy, UCLA, PAB 430 Portola Plaza, Box 951547, Los Angeles, CA 90095-1547

²⁷Jet Propulsion Laboratory, California Institute of Technology, 4800 Oak Grove Drive, Pasadena, CA 91001, USA

²⁸Department of Astronomy and Astrophysics, University of California, Santa Cruz, 1156 High Street, Santa Cruz, CA 95064, USA

²⁹Institute for Astronomy, University of Hawai'i at Manoa, 2680 Woodlawn Drive, Honolulu, HI 96822, USA

³⁰Department of Astronomy, School of Science, The University of Tokyo, 7-3-1 Hongo, Bunkyo, Tokyo 113-0033, Japan

ABSTRACT

The *James Webb Space Telescope* (*JWST*) is opening new frontiers of transient discovery and follow-up at high-redshift. Here we present the discovery of a spectroscopically confirmed Type Ia supernova (SN Ia; SN 2023aeax) at $z = 2.15$ with *JWST*, including a NIRC*am* multi-band light curve. SN 2023aeax lands at the edge of traditional low- z cosmology cuts because of its blue color (peak rest-frame $B - V \sim -0.3$) but with a normal decline rate ($\Delta m_{15}(B) \sim 1.25$), and applying a fiducial standardization with the BayeSN model we find the SN 2023aeax luminosity distance is in $\sim 0.1\sigma$ agreement with Λ CDM. SN 2023aeax is only the second spectroscopically confirmed SN Ia in the dark matter-dominated Universe at $z > 2$ (the other is SN 2023adsy), giving it rare leverage to constrain any potential evolution in SN Ia standardized luminosities. Similar to SN 2023adsy ($B - V \sim 0.8$), SN 2023aeax has a fairly extreme (but opposite) color, which may be due to the small sample size or a secondary factor, such as host galaxy properties. Nevertheless, the SN 2023aeax spectrum is well-represented by normal low- z SN Ia spectra and we find no definitive evolution in SN Ia standardization with redshift. Still, the first two spectroscopically confirmed $z > 2$ SNe Ia have peculiar colors and combine for a $\sim 1\sigma$ distance slope relative to Λ CDM, though in agreement with recent SN Ia cosmological measurements.

1. INTRODUCTION

Luminosity distances measured from Type Ia supernovae (SNe Ia) have led to the inferred existence of dark energy (Riess et al. 1998; Perlmutter et al. 1999), our most precise local measurement of the Hubble constant (H_0 Riess et al. 2022), and have constrained numerous astrophysical quantities (e.g. the rate of light and intermediate elements, nucleosynthesis, etc). SNe Ia will continue to refine our understanding of dark energy through upcoming missions such as the Rubin Observatory Legacy Survey of Space and Time (LSST) and *Roman Space Telescope* High Latitude Time Domain Survey (HLTDS), which will use large numbers of SNe Ia discovered over a wide redshift range ($z \lesssim 3$; Hounsell et al. 2018; Ivezić et al. 2019; Rose et al. 2021; Mitra et al. 2023) to measure changes in dark energy over time.

Current measurements of evolving dark energy require that the standardization properties of SNe Ia do not change with redshift, as such a signal could falsely mimic a change in dark energy. However, SN Ia luminosity evolution is a distinct possibility as many redshift-evolving global properties could plausibly impact SN Ia luminosities (e.g., metallicity, dust; Moreno-Raya et al. 2016; Brout & Scolnic 2021). As dark energy is not expected to vary significantly in the dark-matter dominated universe beyond $z \sim 2$, high- z SNe Ia have unique leverage on these potential SN Ia systematics (Riess & Livio 2006; Lu et al. 2022). If luminosity distances measured from SNe Ia at $z \gtrsim 2$ diverge from expectations (i.e., existing cosmological measurements; Scolnic et al. 2018; Brout et al. 2022; DES Collaboration et al. 2024), it would strongly indicate the existence of intrinsic SN Ia luminosity evolution (for example, see Moreno-Raya et al. 2016) or highly non-standard cosmological model, instead of variable dark energy.

Detecting SNe Ia at $z \gtrsim 2$ requires deep ($m_{AB} \gtrsim 26$ per-visit depth) imaging observations in red ($\gtrsim 1.2\mu\text{m}$) filters. While the *Hubble Space Telescope* (*HST*) observed SNe Ia to $z = 2.24$, all SNe Ia beyond $z \sim 1.6$ were strongly lensed (which adds many systematics, see Pierel et al. 2021; Chen et al. 2024; Frye et al. 2024; Pierel et al. 2024b,c; Pascale et al. 2025) and/or photometrically classified (Rodney et al. 2014). Due to both depth and wavelength constraints (e.g., Filippenko 1997), spectroscopic confirmation of SNe Ia at $z > 2$ was simply not possible before the arrival of the *James Webb Space Telescope* (*JWST*). Since its launch, the sensitivity and wavelength coverage of *JWST* has allowed it to consistently make detections and spectroscopic classifications of high- z SNe ($z \lesssim 4$; Engesser et al. 2022a,b; DeCoursey et al. 2023b, 2024; Pierel et al. 2024b,c,d; Siebert et al. 2024; Coulter et al. 2025), revolutionizing our view of the high- z transient universe.

The first spectroscopically confirmed SNIa at $z > 2$, SN 2023ad_{sy}, was recently discovered and followed with *JWST* (DeCoursey et al. 2024; Pierel et al. 2024d). SN 2023ad_{sy} was classified both spectroscopically and photometrically as a SNIa, with a spectroscopic redshift of $z = 2.903$, but with some peculiarities. In particular, the SN was extremely red (rest-frame color $B - V \sim 0.8$, compared to normal low- z SNe Ia $-0.4 \lesssim B - V \lesssim 0.2$) with a high Ca II velocity $\sim 19,000$ km/s relative to the normal population of SNe Ia. Spectral energy distribution (SED) modeling of the SN host template photometry show the galaxy is fairly low-mass ($\sim 10^8 M_\odot$), low-metallicity ($\sim 0.3Z_\odot$), and low-extinction ($A_V < 0.1$), suggesting the SN may be intrinsically red. Using traditional standardization methods (e.g., Guy et al. 2007; Betoule et al. 2014; Scolnic et al. 2018; Kenworthy et al. 2021; Pierel et al. 2022) resulted in a SN 2023ad_{sy} luminosity distance $\sim 1\sigma$ above Λ CDM (Pierel et al. 2024d). Thus the properties of SN 2023ad_{sy} suggest that SN Ia population characteristics may be changing with redshift (i.e., changes in the progenitor system may lead to systematically redder, Ca-rich SNe Ia, see Woosley et al. 1986; Bildsten et al. 2007; Perets et al. 2010; Shen et al. 2010; Waldman et al. 2011; Kasliwal et al. 2012; Foley 2015; De et al. 2020; Zenati et al. 2023), and the stability of their standardization is still uncertain to $z \sim 3$. SN 2023ad_{sy} is the first spectroscopically confirmed SNIa at $z > 2$, and thus a larger sample is needed to determine if SN 2023ad_{sy} is representative or peculiar for high- z SNe Ia and to conclusively determine if their standardization evolves with redshift.

A candidate for the second confirmed non-strongly lensed SNIa at $z > 2$ has been found in *JWST* imaging conducted as part of the *JWST* Cosmic Evolution Survey (COSMOS-Web; Casey et al. 2023) program. COSMOS-Web observed 0.54 deg^2 of sky to single-visit 5σ depths of $m_{AB} \sim 28$ in 4 NIRC_{am} filters in January 2024, overlapping with $148^{\prime 2}$ of imaging (containing 8 NIRC_{am} filters) from the Public Release IMaging for Extragalactic Research (PRIMER; Dunlop et al. 2021) program taken in Spring 2023. This repeated imaging gave a sufficiently long baseline to search for transient objects with sensitivity for SNe Ia to $z > 3$. Of the dozens of detected transient objects (A. Rest et al., in preparation), one (subsequently named SN 2023ae_{ax} and found in a galaxy at R.A. = 10h00m26.3911s decl. = +02d19m34.077s), was identified by its colors, photometric redshift, and luminosity as a possible SNIa candidate at $z \sim 2.3$. A *JWST* Director’s Discretionary Time (DDT) program was approved to follow-up the most interesting transients in the field (Coulter et al. 2024), providing an additional imaging epoch and a spectrum for several SNe including SN 2023ae_{ax}, which received a refined redshift of $z = 2.15 \pm 0.01$ based on the spectrum.

Here we describe the classification and analysis of SN 2023ae_{ax}, beginning with a summary of the observations in Section 2 and followed by a spectroscopic classification in Section 3. Light curve fitting and the subsequent standardized distance measurement are completed in Section 4, and

* NASA Einstein Fellow

† ISEF International Fellowship

we conclude in Section 5 with a discussion of the implications of SN 2023aeax for SN Ia cosmology and the future of high- z SN Ia observations with *JWST*. In this analysis, we assume a standard flat Λ CDM cosmology with $H_0 = 70 \text{ km s}^{-1} \text{ Mpc}^{-1}$, $\Omega_m = 0.315$.

2. SUMMARY OF OBSERVATIONS

SN 2023aeax was observed in a total of three *JWST* visits spanning ~ 200 observer-frame days. The method for detecting SNe and the subsequent DDT program observations are described in detail by A. Rest et al., in preparation (hereafter R24). Briefly, SN 2023aeax was detected in COSMOS-Web observations (Program ID [PID] 1727) taken on 2023 December 27 (MJD ~ 60305) using the F115W, F150W, F277W, F444W filters. These overlapped with observations from the PRIMER program (Dunlop et al. 2021) taken in the observing window 2023 May 6-18 (MJD ~ 60076), a baseline of ~ 2.5 rest-frame months for SN 2023aeax. A *JWST* DDT program (PID 6585 Coulter et al. 2024) was approved to follow the most interesting transients with a visit on 2024 April 29 (MJD 60429), including nearly seven hours of integration in the NIRSpec (Jakobsen et al. 2022) multi-object spectroscopy (MOS) mode using the micro-shutter assembly (MSA; Ferruit et al. 2022) and low-resolution Prism ($R \sim 100$). The MSA provided SN spectra for several transients, with the others described in companion papers (e.g., D. Coulter et al. in preparation and R24) as well as a variety of galaxy spectra.

After the discovery of SN 2023aeax in COSMOS-Web data, an archival search of *JWST*/NIRCam imaging revealed serendipitous observations by ‘‘A Pure Parallel Wide Area Legacy Imaging Survey at 1-5 Micron’’ (PANORAMIC, PID 2514; Williams et al. 2021) on 2023 December 3 (MJD 60281) in six NIRCam filters, preceding the COSMOS-Web detection image. PANORAMIC therefore provides the first epoch of imaging for SN 2023aeax, and below we describe the data reduction and analysis of the combined dataset.

2.1. Measuring Photometry

We follow the same methods for photometry on Level 3 (drizzled, I2D) *JWST* images as Pierel et al. (2024d). Level 3 NIRCam images are the drizzled and resampled combination of Level 2 (CAL) NIRCam images. CALs are individual exposures that have been calibrated using the STScI *JWST* Pipeline¹ (Bushouse et al. 2022), and have been bias-subtracted, dark-subtracted, and flat-fielded but not yet corrected for geometric distortion.

We first align the individual NIRCam exposures containing SN 2023aeax, from all three programs described above (see Table 1), to the drizzled template images from PRIMER, as PRIMER provides a temporal reference image in all filters where SN 2023aeax was observed. We use the *JWST*/*HST* Alignment Tool (JHAT; Rest et al. 2023)², which improves

the relative default alignment from ~ 1 pixel to ~ 0.1 pixel between the epochs.

We produce aligned drizzled images with the *JWST* pipeline (v1.12.5; Bushouse et al. 2022), and obtain difference images in all filters (Figure 1) using the High Order Transform of PSF and Template Subtraction (HOTPANTS; Becker 2015)³ code (with modifications implemented in the photpipe code; Rest et al. 2005). We implement the space_phot (Pierel 2024)⁴ drizzled PSF fitting routine using 5×5 pixel cutouts and Level 2 PSF models from webbpsf⁵, which are temporally and spatially dependent and include a correction to account for the finite PSF size. The Level 2 PSF models are drizzled together using the same pipeline implementation as the data, and fit to the observed SN 2023aeax flux. These total fluxes, which are in units of MJy/sr, are converted to AB magnitudes using the native pixel scale of each image ($0.03''/\text{pix}$ for SW, $0.06''/\text{pix}$ for LW). Measured photometry is given in Table 1. A final source of photometric uncertainty is a systematic uncertainty on the zero-points, which is $\lesssim 0.01$ mag for all filters and is therefore subdominant to the uncertainties derived here (M. Boyer 2024, private communication; M. Boyer et al., in preparation).

2.2. NIRSpec Reduction

We began processing the spectroscopic data with Stage 2 products from the Mikulski Archive for Space Telescopes (MAST). Additional processing used the *JWST* pipeline (v1.12.5; Bushouse et al. 2022)⁶ to produce two-dimensional (2D) spectral data (Figure 2). The pipeline applied a slit-loss throughput correction for SN 2023aeax based on the planned position of a point-source within the MSA shutters (Figure 2). The 2D spectrum of SN 2023aeax and its host galaxy was extracted using the optimal extraction algorithm from Horne (1986) implemented as scripts available as part of the MOS Optimal Spectral Extraction (MOSE) notebook⁷. To separate the spectrum of SN 2023aeax and its host galaxy we extract a 1D spectrum from each of the rows neighboring the trace associated with SN 2023aeax, which creates a spectrum of the host galaxy from the region local to the SN. We then subtract this host galaxy spectrum from the combined extraction to obtain a 1D spectrum for SN 2023aeax, with each of these stages shown in Figure 3. We discuss the effectiveness of this method in the next section.

3. CLASSIFICATION AS TYPE IA

There are no clear [OIII] (rest-frame $5,007\text{\AA}$) or $H\alpha$ ($6,563\text{\AA}$) emission lines in the host galaxy spectrum (Figure 3), making a precise spectroscopic redshift measurement im-

¹ <https://github.com/spacetelescope/jwst>

² <https://jhat.readthedocs.io>

³ <https://github.com/acbecker/hotpants>

⁴ space-phot.readthedocs.io

⁵ <https://webbpsf.readthedocs.io>

⁶ With context file jwst_1183.pmap

⁷ https://spacetelescope.github.io/jdat_notebooks/notebooks/ifu_optimal/ifu_optimal.html

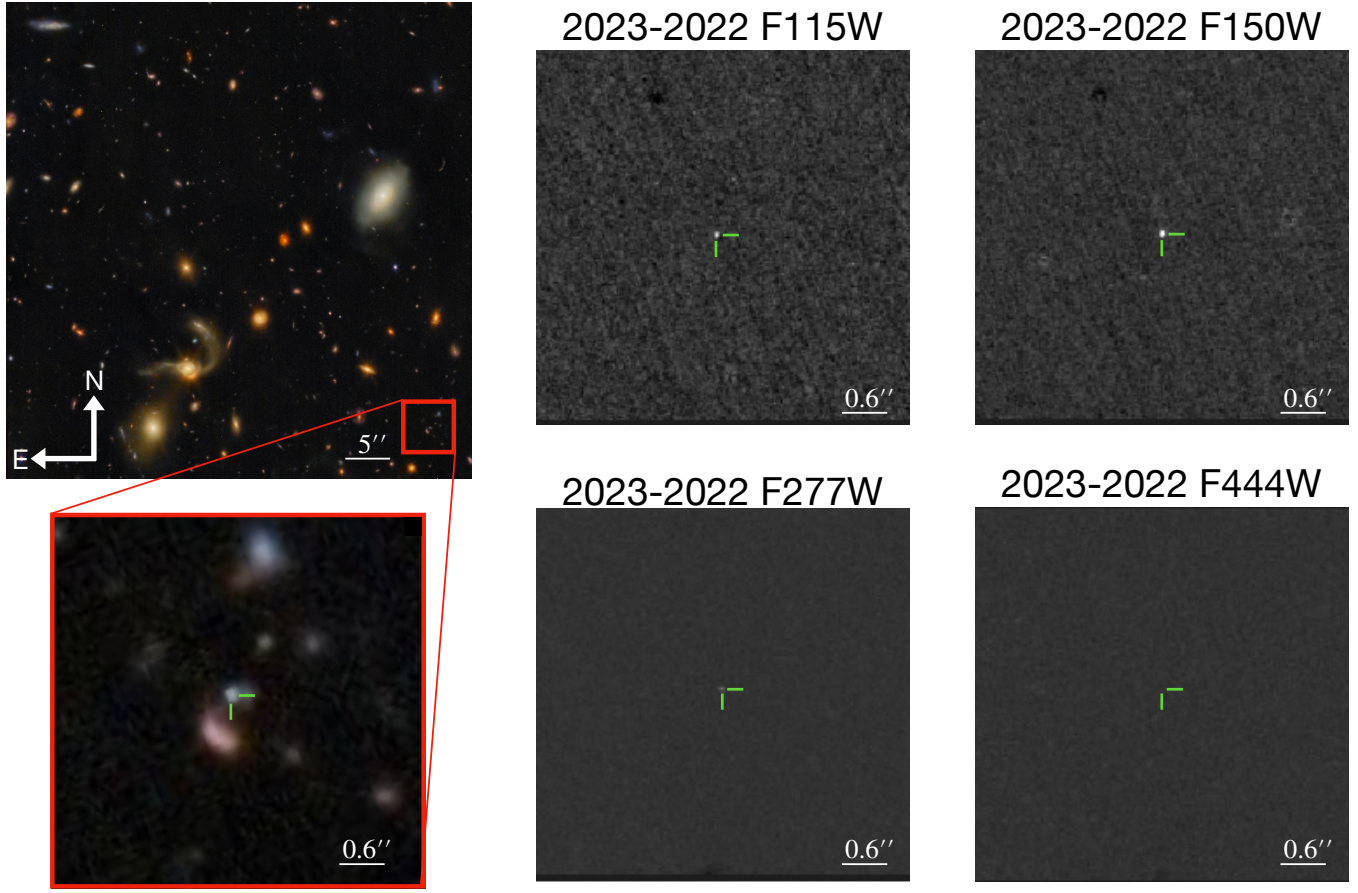


Figure 1. (Left column) Full-color images (from PID 2514) using F115W+F150W (Blue) F200W+F277W (Green) and F356W+F444W (Red), with a zoomed-out view on the top and the host of SN 2023aeax on the bottom. (Column 2-3) Difference images created from the COSMOS-Web and PRIMER visits separated by ~ 1 year, with the SN 2023aeax position marked with a green indicator. All images are drizzled to $0.03''/\text{pix}$ and the cutouts have the same spatial extent.

possible. We therefore first fit the template host photometry, which was measured from observations taken in 2022 by the PRIMER program (Dunlop et al. 2021) as well as earlier optical *HST* imaging from COSMOS (Koekemoer et al. 2007) and CANDELS (Grogin et al. 2011; Koekemoer et al. 2011), and *Spitzer* mid-IR imaging, with the EAZY software package (Brammer et al. 2008). The SED was well sampled, and provided a robust photo- z posterior with a 68th-percentile range of $1.91 < z < 2.29$, with a best-fit of $z = 2.25$. Other basic properties of the host from the SED fit are given in Table 2, derived after fixing the redshift based on the analysis below. The properties show a relatively low-mass quiescent galaxy, which is expected for an SN Ia.

We use the Next Generation SuperFit (NGSF; Goldwasser et al. 2022)⁸ package to classify SN 2023aeax. NGSF matches a database of reference SN spectra for a variety of SN types to the observed spectrum, while varying levels of dust extinction and host galaxy contamination. We allow the redshift to vary in the 1σ range of the photo- z for the host

galaxy ($1.9 < z < 2.3$). Of the top ten reference SN spectra matched to the SN 2023aeax spectrum, eight are of normal SNe Ia and the remainder are the 91T SN Ia sub-type (e.g., Fisher et al. 1999), with the best match being the normal SN Ia 2011by at +52 rest-frame days relative to peak B-band brightness (e.g., Foley & Mandel 2013; Graham et al. 2015; Foley et al. 2020). A variety of normal and peculiar SN Ia sub-types fill the top 40 matched reference spectra, before core-collapse subtypes appear.

Figure 4 shows the best spectral template match for SN Ia, SN Ia 91T-like, and three core-collapse sub-types (IIP, Ib, Ic). All templates show a 8300\AA Ca II absorption, but the shape of the absorption is best-matched by the SN Ia sub-types. The 6150\AA Si II feature is also present in both SN Ia sub-type templates as well as the SN 2023aeax spectrum, but not the core-collapse sub-types. Additionally, there are a variety of features present in the various core-collapse sub-types not present in the SN 2023aeax spectrum. Overall, the SN Ia spectral template match provides a χ^2 per degree of freedom (ν) of 2.30, while the next best (non-normal SN Ia) fit is a 91T-like SN Ia with 3.40 (Table 3).

⁸ <https://github.com/oyaron/NGSF>

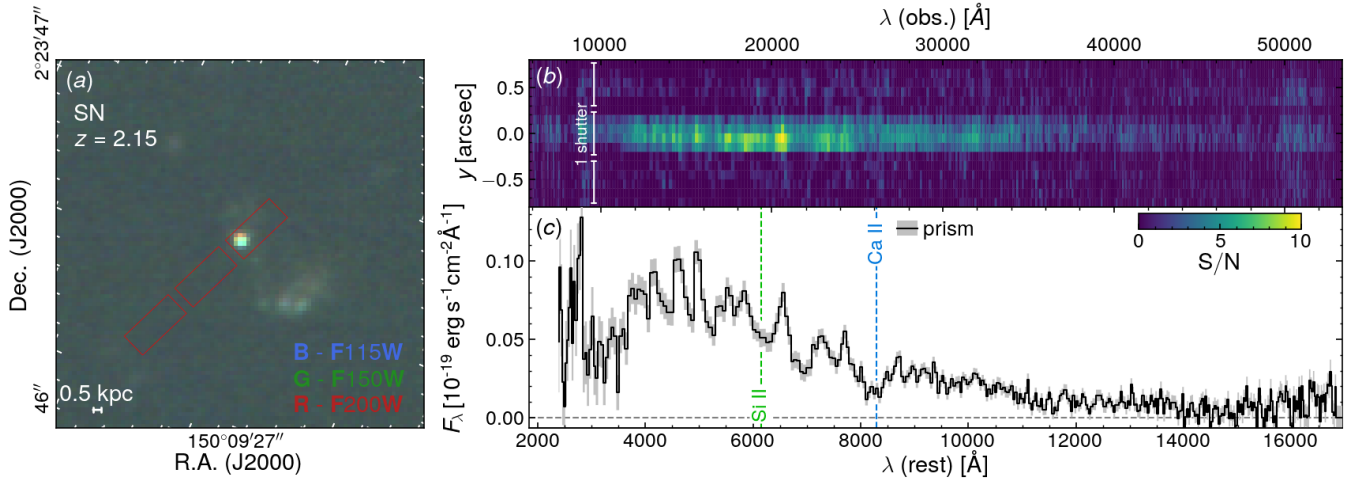


Figure 2. (a) The NIRSpect/MSA slitlet positions over SN 2023aeax for one of the dithered observations. (b,c) The 2D and 1D-extracted NIRSpect spectrum for SN 2023aeax. The two absorption lines primarily used for spectroscopic classification of SNe Ia, are shown with dotted lines.

Table 1. Observations for SN 2023aeax discussed in Section 2.

PID	MJD	Instrument	Filter/Disperser	m_{AB}
1837	60061	NIRCam	F115W	—
1837	60061	NIRCam	F150W	—
1837	60061	NIRCam	F200W	—
1837	60061	NIRCam	F277W	—
1837	60061	NIRCam	F356W	—
1837	60061	NIRCam	F444W	—
2514	60281	NIRCam	F115W	25.69 ± 0.05
2514	60281	NIRCam	F150W	25.34 ± 0.04
2514	60281	NIRCam	F200W	25.42 ± 0.04
2514	60281	NIRCam	F277W	26.50 ± 0.06
2514	60281	NIRCam	F356W	27.24 ± 0.12
2514	60281	NIRCam	F444W	27.45 ± 0.25
1727	60305	NIRCam	F115W	26.49 ± 0.11
1727	60304	NIRCam	F150W	26.00 ± 0.06
1727	60303	NIRCam	F277W	27.10 ± 0.09
1727	60302	NIRCam	F444W	> 28.5
6585	60429	NIRCam	F115W	28.97 ± 0.26
6585	60429	NIRCam	F150W	28.08 ± 0.09
6585	60429	NIRCam	F277W	28.34 ± 0.19
6585	60429	NIRCam	F444W	> 28.6
6585	60429	NIRSpect	Prism	—

NOTE—Columns are: *JWST* Program ID, Modified Julian date, *JWST* instrument, filter or grating, and photometry plus final uncertainty for SN 2023aeax. Upper limits are 5σ . PID 1837 is PRIMER, 2514 is PANORAMIC, 1727 is COSMOS-Web, and 6585 is the DDT program. Each magnitude is measured using a difference image with PRIMER (PID 1837).

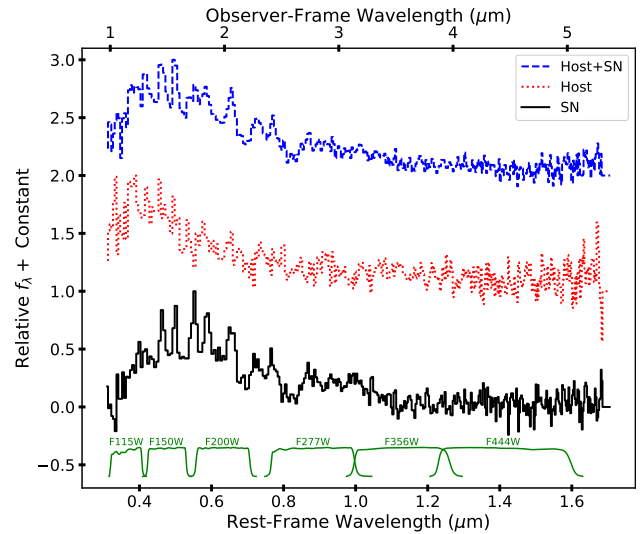


Figure 3. The raw combined Host+SN spectrum is shown as a blue dashed line (top), followed by the host spectrum as a red dotted line extracted from rows neighboring the SN trace in Figure 2 (middle), and the host-subtracted SN spectrum is a black solid line (bottom). The black line is used for spectroscopic classification, and no obvious spectroscopic emission features are present for a redshift in the host spectrum. The NIRCams filters used here are shown in green at the bottom of the figure for reference.

Table 3 also contains the inferred time of peak B-band brightness for SN 2023aeax, based on the phase of the best-fit spectral template for each SN sub-type. From the light curve fitting in Section 4, it is clear that the time of peak brightness must be before MJD 60305 (as the epoch at 60281 is brighter), a condition that is only met by the SN Ia and 91T-like templates. In other words, if SN 2023aeax would be a core-collapse SN, then based on the spectrum it would need to be younger than what is possible given the light curve (Section 4). Of the two SN Ia classes, a normal SN Ia is

Table 2. Properties derived from an EAZY fit to the host SED. The redshift was measured before follow-up, the other properties after fixing the redshift to $z = 2.15$ given this analysis.

Property	Best-fit
z	$2.25^{+0.04}_{-0.34}$
$\log M_*/M_\odot$	8.1 ± 0.1
$\log Z_*/Z_\odot$	-1.0 ± 0.3
$\log \text{sSFR}$	-8.2 ± 0.2
A_V	$0.2^{+0.2}_{-0.1}$

NOTE—Columns are: Host property and best-fit measurement with uncertainty. The measured properties are redshift, mass, metallicity, specific star formation rate, and V-band dust extinction. The redshift is that measured before follow-up using the PRIMER SED (setting the prior for this analysis), while the remaining properties are derived after setting the redshift to $z = 2.15$ based on this analysis.

strongly preferred given the significantly lower χ^2/ν (Table 3). Additionally, the light curve decline rate is more consistent with a normal SN Ia (see Section 4.1; Dimitriadis et al. 2024), so we therefore proceed with the classification of normal SN Ia.

We take the median and standard deviation in redshift for the top ten SN Ia spectral matches as the final redshift measurement for SN 2023aeax, which is 2.15 ± 0.01 . We also note that NGSF provides an estimate of the fraction of flux in the spectrum associated with the SN relative to the host galaxy. Running NGSF on the blue spectrum in Figure 3 decreases the SN flux contribution of the top matches to $\sim 40\%$ from $\gtrsim 90\%$ (for the black spectrum) while improving the χ^2/ν , giving some evidence of the effectiveness of the method.

4. LUMINOSITY DISTANCE MEASUREMENT

4.1. Light Curve Fitting

We begin by fitting the observed photometry (including upper-limits; Table 1) with a phase-extended version of the BayeSN SN Ia SED model (Mandel et al. 2022; Grayling et al. 2024), which covers the full plausible rest-frame phase range of SN 2023aeax, to fit the measured photometry. The version of BayeSN we use is a variant of the one presented by Ward et al. (2023) and uses the training set detailed therein. The model is trained to cover rest-frame phases as late as 50 days after peak-brightness with linear extrapolation in the space of the logarithm of the SED beyond that. This is the same model used by Pierel et al. (2024b) to successfully fit a (strongly lensed) SN Ia at $z = 1.78$, and is the only current light curve model with the phase and wavelength range needed to fit these data.

In addition to the base template, BayeSN includes a rest-frame host-galaxy dust component (parameterized by the V-band extinction A_V and ratio of total to selective extinc-

Table 3. The time of peak B-band brightness (t_{pk}) inferred from the best spectral template match for each SN type, and the resulting reduced χ^2 .

SN Type	Best t_{pk}	χ^2/ν
Ia	60265	2.30
Ia-91T	60171	3.40
Ib	60374	8.37
Ic	60391	5.52
IIP	60321	5.57

NOTE—Columns are: SN type model/spectral template used, the time of peak B-band brightness given the best-fit spectroscopic template match, and the χ^2 per DOF of the best-fit spectroscopic template match. Note that given the temporal separation between detection and obtaining the spectrum of SN 2023aeax the time of peak brightness must be $\text{MJD} < 60305$, which is only satisfied by SN Ia and Ia-91T with a statistical preference for normal SN Ia.

Table 4. The BayesN light curve model parameters used in this analysis.

Parameter	Best-Fit
z	2.15 (Fixed)
t_{pk} (MJD)	$60270.34^{+2.89}_{-2.23}$
A_V	< 0.04
θ	$-0.52^{+0.33}_{-0.36}$
μ	$46.10^{+0.14}_{-0.12}$

NOTE—Columns are: BayeSN parameter, and fitted result with uncertainty. Note that the fitted A_V is approaching the physical lower bound of 0, and so we report the 1σ upper-limit. The uncertainty on μ includes only model and statistical uncertainties, with more added in Section 4. The best-fit MJD corresponds to November 22, 2023.

tion R_V) and a light curve shape parameter θ (This has a strong negative correlation with the SALT2 light curve model stretch parameter, x_1 , meaning positive θ implies a faster decline rate; see e.g., Figure 4 of Mandel et al. 2022). We add a 0.01 mag Galactic extinction correction to the model based on the dust maps of Schlafly & Finkbeiner (2011) and using the extinction curve from Fitzpatrick (1999). The BayeSN “ ϵ -surface” captures all additional model/intrinsic scatter and intrinsic color variation. Finally, BayeSN directly infers the luminosity distances as part of the Bayesian inference process. The best-fit model is shown with the observed photometry in Figure 5, and the retrieved BayeSN parameters from the fit are shown in Table 4, with the posterior distributions shown in Figure 6. Note that the fit for A_V , the extrinsic dust, approaches the physical lower bound of 0. This suggests little to no dust extinction for SN 2023aeax (in

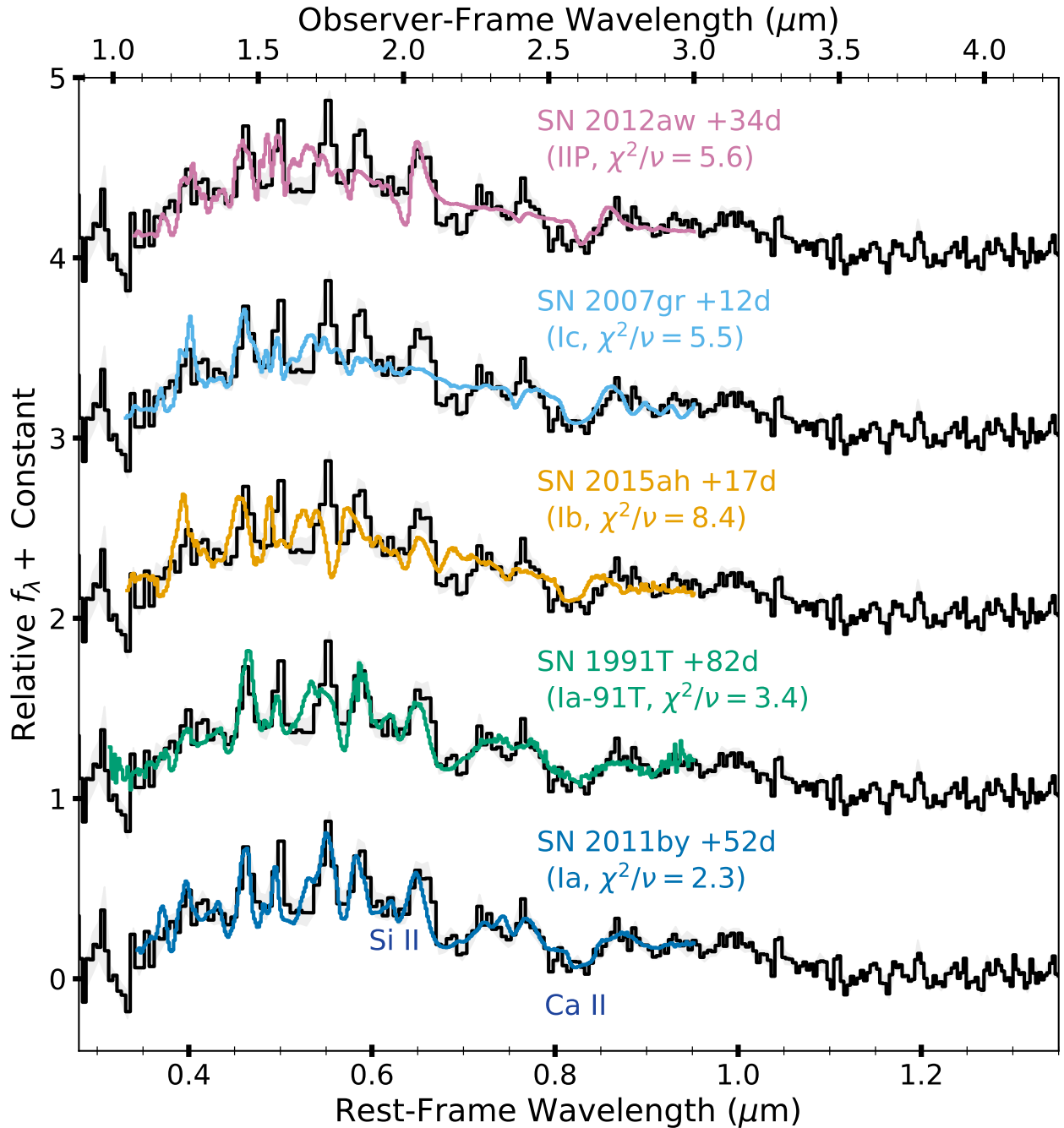


Figure 4. The host-subtracted NIRSpec spectrum (with uncertainty) of SN 2023aeax is shown as a black solid line, with the primary features used for the preferred SN Ia classification labeled (bottom). The best-match template from NGSF is a SN Ia (blue, +52d, bottom), and a 91T-like SN Ia subclass (green, +82d, second from bottom) is also shown for comparison. The best core-collapse matches are also shown, including Ib (yellow, third from top), Ic (cyan, second from top), and IIP (pink, top). A normal SN Ia is heavily favored based on the spectrum (see Table 3). All phases are rest-frame days relative to peak B-band brightness.

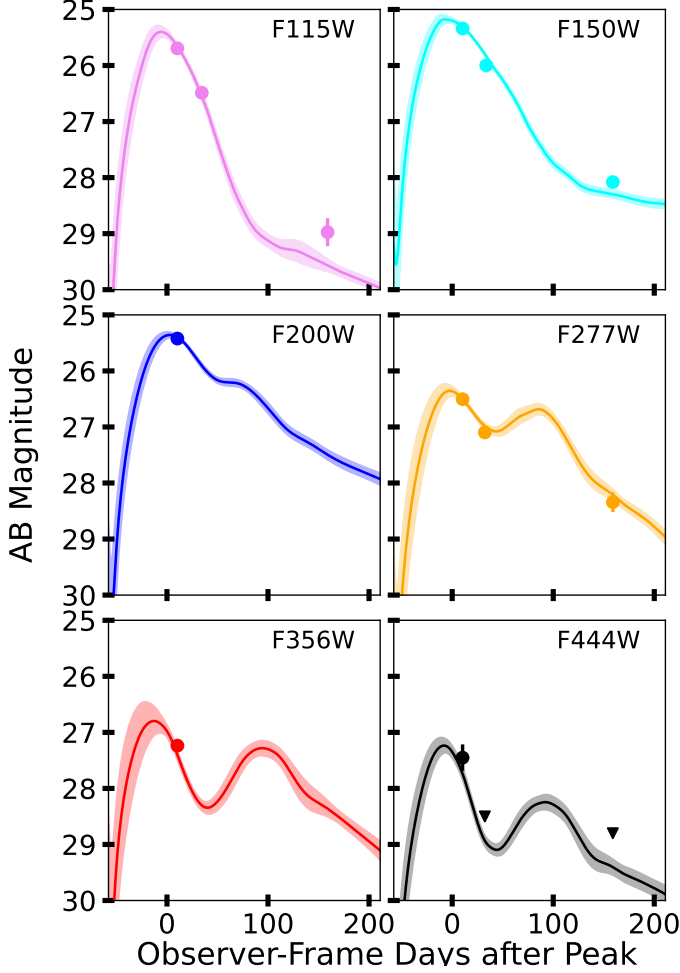


Figure 5. The photometry measured in Section 2.1 is shown as black circles with error, with (5σ) upper-limits denoted by triangles. The fit to the full light curve is shown as a solid line in each filter, with the shaded region representing the BayeSN model+fitting uncertainty. The time of peak brightness is measured relative to the rest-frame B-band and is reported in Table 4, and the amplitude is set by the luminosity distance (Section 4.1).

agreement with the host SED fitting in Table 2), but as this is not a reliable constraint on A_V we report the 1σ upper-limit (0.04). The value of θ corresponds to a $\Delta m_{15}(B)$ of $\sim 1.25 \pm 0.09$, which is well-within the normal low- z SN Ia population (Figure 7). The rest-frame $B - V$ color at peak brightness for SN 2023aeax is $-0.3 \pm 0.1\text{mag}$, which is on the blue edge of the normal low- z SN population (see Figure 7), but is just within traditional low- z color cosmology cuts ($-0.4 \lesssim B - V \lesssim 0.4$, or using the SALT “ c ” parameter $-0.3 < c < 0.3$; Brout et al. 2022).

4.2. Adding SN 2023aeax to the Hubble Diagram

As noted in the previous section, BayeSN infers the luminosity distance for a SN Ia directly as a result of its Bayesian model fitting step. The only additional corrections to this value would be a bias correction (e.g., Kessler & Scolnic

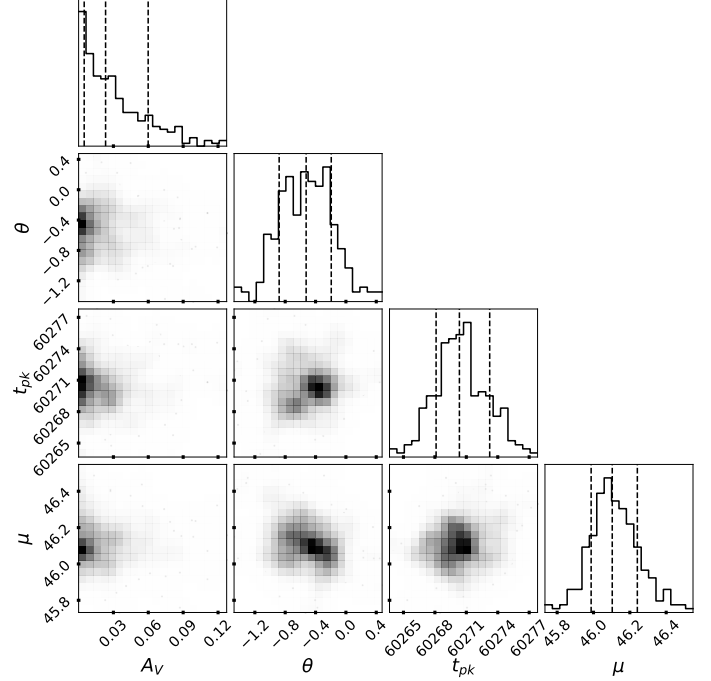


Figure 6. Posterior distributions for the BayeSN fitting of SN 2023aeax photometry. The dashed vertical lines correspond to the distribution 16th, 50th, and 84th quantiles. The parameters are V -band dust extinction, light curve shape, time of peak B-band brightness, and distance modulus.

2017) and a correction for the host-galaxy mass step, or the small residual correlation between SN Ia distance measurements and their host-galaxy masses that may be driven by interstellar medium (ISM) dust mass surface density (Kelly et al. 2010; Lampeitl et al. 2010; Sullivan et al. 2010; Brout & Scolnic 2021). The nature and evolution of the host-galaxy mass step is unknown, especially at such high redshift (e.g., Childress et al. 2014), and its correction to a BayeSN distance measurement is not well-understood. We simply apply half of the host mass step (for a low-mass galaxy, Table 2) from Brout et al. (2022) (who found $\sim 0.054\text{mag}$) as a systematic error in quadrature. As for the selection bias correction, Pierel et al. (2024d) explored this with extensive simulations for an SN Ia also discovered at $z > 2$ by *JWST*. SN 2023aeax is several magnitudes brighter than the survey limiting magnitude, and in this case the fitted light curve parameters are within normal ranges, meaning that a bias correction is not necessary in this instance. Once a larger sample of $z > 2$ SNe Ia are found, a population-level analysis will be warranted to account for biases (e.g., Scolnic et al. 2018; Brout et al. 2022).

The final luminosity distance measurement is $46.10^{+0.17}_{-0.18}$ mag, while the ΛCDM prediction at $z = 2.15$ (with $H_0 = 70 \text{ km s}^{-1} \text{ Mpc}^{-1}$) is $\mu = 46.12$ mag, a $\ll 1\sigma$ difference (Figure 8). The uncertainty on μ includes the fitted model uncertainties, errors from redshift and peculiar velocity (which are negligible here), and an additional $0.055z$ mag

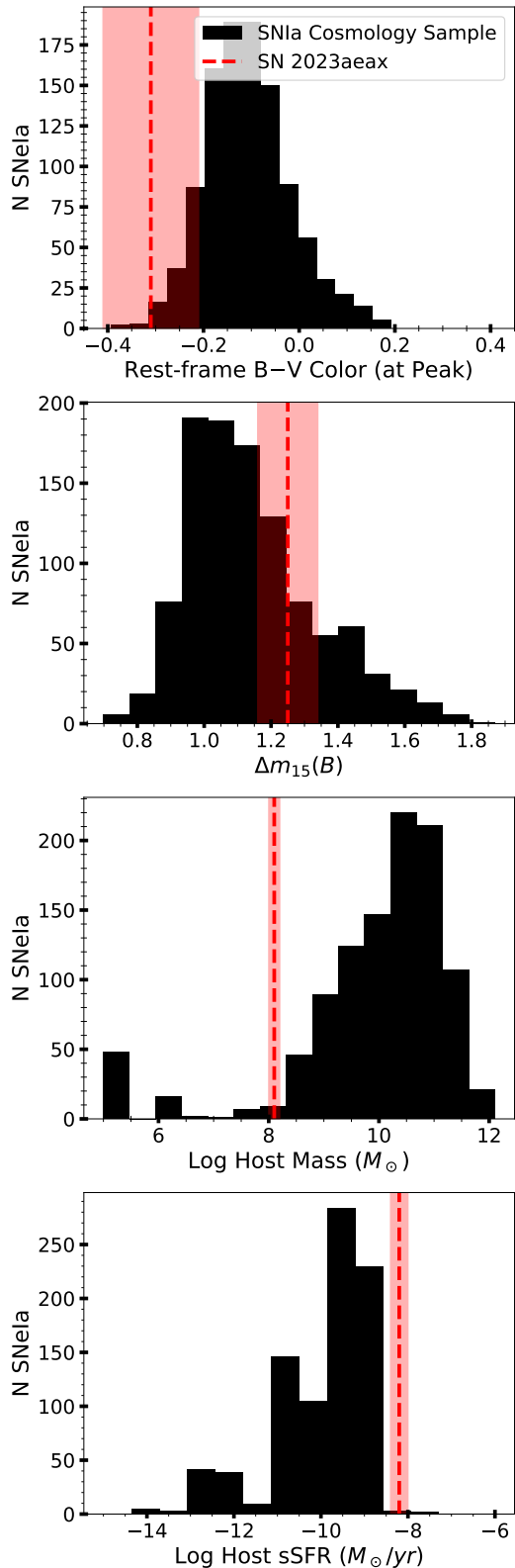


Figure 7. The distributions of rest-frame $B-V$ color at peak B-band brightness, $\Delta m_{15}(B)$, and host galaxy properties measured for the cosmological sample of SNe Ia presented in Brout et al. (2022). The vertical red dashed lines are the measurements for SN 2023aeax.

uncertainty from weak gravitational lensing (Jönsson et al. 2010). SN 2023aeax is only the second spectroscopically classified non-strongly lensed SN Ia at $z > 1.6$, and while its distance modulus agrees with Λ CDM the combination of $z < 2$ SNe Ia and SN 2023adsy with SN 2023aeax suggests a possible slope (at $\sim 1\sigma$ relative to Λ CDM) in SN Ia luminosity distance measurements as a function of redshift. This trend is well-within the best current cosmological constraints from SNe Ia (Brout et al. 2022; DES Collaboration et al. 2024), which are shown in Figure 8. We note that the SN 2023adsy luminosity distance was measured with SALT3-NIR (Pierel et al. 2022), but we re-fit the published photometry (including the $> 4\mu\text{m}$ data) following our methodology here and find excellent agreement between the two models ($47.14^{+0.21}_{-0.24}$ compared to $47.18^{+0.27}_{-0.28}$). In Figure 8, we show the SN 2023adsy distance modulus measured in this work alongside SN 2023aeax for reference.

5. DISCUSSION

We have presented *JWST* observations of a SN (SN 2023aeax) with a redshift of $z = 2.15 \pm 0.01$, which we classify using a NIRSpec spectrum as a SN Ia. Using the BayeSN SN Ia standardization model that has been used successfully at lower redshift ($z \lesssim 2$), we measure the luminosity distance to SN 2023aeax. We find a value of $\mu = 46.10^{+0.17}_{-0.18}$ mag, which is in 0.1σ agreement with Λ CDM. Although more objects are needed to directly constrain cosmological parameters at high- z , any significant deviation of SN Ia luminosity distances from Λ CDM at $z > 2$ (in the dark matter-dominated universe) would be a strong indicator of SN Ia luminosity evolution with redshift or evidence for a more exotic cosmological model. Such a test is only newly possible with *JWST*, the only telescope capable of robust spectroscopy of SNe Ia in the dark matter-dominated universe. While SN 2023aeax is in excellent agreement with Λ CDM, combining this SN with previous $z < 2$ SNe Ia and SN 2023adsy at $z = 2.903$ results in a $\sim 1\sigma$ slope relative to Λ CDM but well within current constraints from Brout et al. (2022) and DES Collaboration et al. (2024), and so a larger sample needed to determine the validity of this result.

SN 2023aeax is just the second spectroscopically confirmed, non-gravitationally lensed SN Ia at $z > 2$ (the other is SN 2023adsy at $z = 2.903$), and the first with light curve properties that would pass low- z cosmology cuts. The phase of our NIRSpec spectrum does not allow a direct comparison of spectral features between SN 2023aeax and SN 2023adsy, but we can compare light curve properties. We have fit both SNe Ia with BayeSN for direct comparison, removing the possibility of a model bias, resulting in a small slope from $z < 2$ to $z \sim 3$ at low confidence ($\sim 1\sigma$). The SNe have normal light curve decline rates ($\Delta m_{15}(B) = 1.25 \pm 0.09$ for SN 2023aeax), but SN 2023adsy had a peculiarly red color (rest-frame $B-V$ of ~ 0.8) that was not easily attributable to dust attenuation, compared to the peak rest-frame $B-V$ color for SN 2023aeax of -0.3 ± 0.1 . We require a larger population of high- z SNe Ia to determine if there are significant changes to the SN Ia population properties between

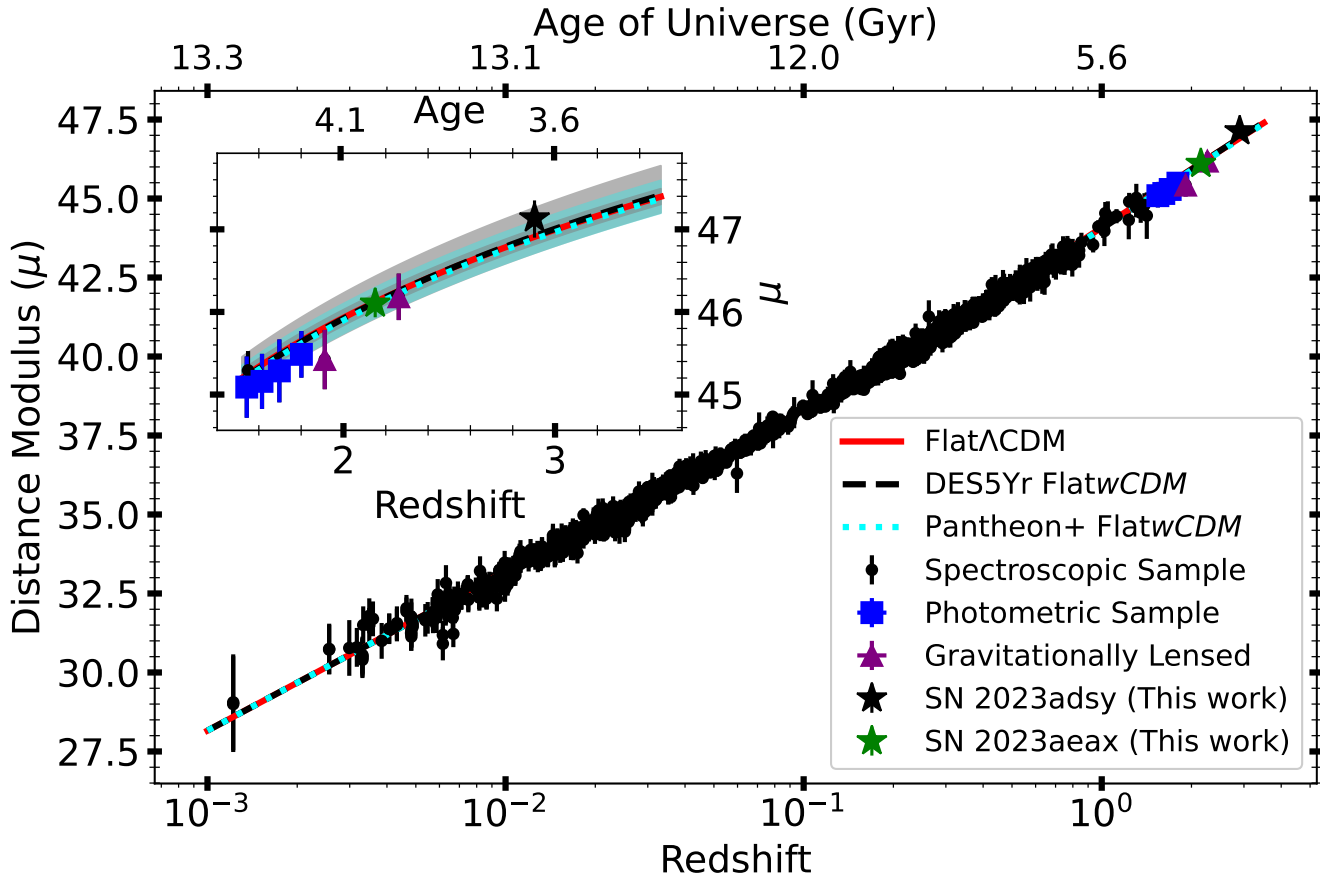


Figure 8. Luminosity distance measurements from the full sample of SNe Ia from Brout et al. (2022) extending to $z = 2.22$. Black points (with errors) are SNe Ia with spectroscopic classifications, while blue squares (with error) are SNe Ia with photometric classifications. The two strongly lensed SNe Ia with distance measurements are shown as purple triangles. SN 2023aeax is shown as a green star, and Λ CDM is shown as a solid red line. The width of the red line encompasses the width of the current H_0 tension, with the center of the line used for reference. The black star is the distance modulus for SN 2023adsy measured in this work with photometry from Pierel et al. (2024d). The best-fit Flat w CDM cosmological constraints from Brout et al. (2022) (black-dashed) and DES Collaboration et al. (2024) (cyan-dotted) are also shown for comparison.

$z = 2.15$ and $z = 2.9$, or if SN 2023adsy is simply an outlier within the high- z SN Ia population. While the peak color of SN 2023aeax is considered just within the cosmological sample for low- z SNe Ia, it is on the extreme blue end, giving another point of consideration as the population of SNe Ia at $z > 2$ grows. The host galaxy properties of SN 2023aeax are also on the edges of, but within, the existing sample of SNe Ia. It is unclear exactly how these properties will evolve with redshift, and such a result is not unexpected.

SN 2023aeax is the second SN Ia with a combined spectroscopic and photometric dataset in the dark matter-dominated universe at $z > 2$, and is the first test for standardized luminosity evolution using a SN Ia that would pass low- z cosmology cuts. Now with a “sample” of two such objects, we find small peculiarities with both that could be indicative of interesting population changes with redshift, or simply statistical fluctuations. The combination of these two SNe Ia from *JWST* with previous work at $z \lesssim 2$ hints at a possible slope in distances with redshift that could be attributed to evolution, with more objects needed to confirm or refute this result. *JWST* is expected to add $\gtrsim 10$ additional such objects over the next two years (Pierel et al. 2024a), and is the only resource capable of doing so before the launch of the *Nancy Grace Roman Space Telescope* (Hounsell et al. 2018; Rose et al. 2021). Regardless, *JWST* will remain the only telescope capable of $z > 2$ SN Ia spectroscopy, and the sample of $\gtrsim 10$ will be required to put valuable constraints on any possible evolution at lower redshift for future cosmological measurements.

Acknowledgements

We would like to thank Matthew Grayling for useful discussion. This paper is based in part on observations with the NASA/ESA Hubble Space Telescope and James Webb Space Telescope obtained from the Mikulski Archive for Space Telescopes at STScI. We thank the DDT and JWST/HST scheduling teams at STScI for extraordinary effort in getting the DDT observations used here scheduled quickly. This work is based on observations made with the NASA/ESA/CSA James Webb Space Telescope. The data were obtained from the Mikulski Archive for Space Telescopes at the Space Telescope Science Institute, which is operated by the Association of Universities for Research in Astronomy, Inc., under NASA contract NAS 5-03127 for JWST. These observations are associated with programs #1727, 1837, 2514, and 6585. This research is based (in part) on observations made with the NASA/ESA Hubble Space Telescope obtained from the Space Telescope Science Institute, which is operated by the Association of Universities for Research in Astronomy, Inc., under NASA contract NAS 5-26555. The JWST data used in this paper can be found in MAST: [10.17909/n7kq-ef83](https://mast.stsci.edu/#/search/10.17909/n7kq-ef83). JDRP is supported by NASA through an Einstein Fellowship grant No. HF2-51541.001 awarded by the Space Telescope Science Institute (STScI), which is operated by the Association of Universities for Research in Astronomy, Inc., for NASA, under contract NAS5-26555. Support was provided to DC, AR, and ME

through program HST-GO-6541. The Cosmic Dawn Center (DAWN) is funded by the Danish National Research Foundation (DNRF140). This work was made possible by utilising the CANDIDE cluster at the Institut d’Astrophysique de Paris. The cluster was funded through grants from the PNCG, CNES, DIM-ACAV, the Euclid Consortium, and the Danish National Research Foundation Cosmic Dawn Center (DNRF140). It is maintained by Stephane Rouberol. M.R.S. is supported by the STScI postdoctoral fellowship. ZGL is supported by the Marsden Fund administered by the Royal Society of New Zealand, Te Apārangi under grant M1255. JS is supported by JSPS KAKENHI (JP22H01262) and the World Premier International Research Center Initiative (WPI), MEXT, Japan. MF is supported by the European Union’s Horizon 2020 research and innovation programme under the Marie Skłodowska-Curie grant agreement No 101148925.

REFERENCES

- Becker, A. 2015, HOTPANTS: High Order Transform of PSF AND Template Subtraction
- Betoule, M., Kessler, R., Guy, J., et al. 2014, *A&A*, 568, A22, doi: [10.1051/0004-6361/201423413](https://doi.org/10.1051/0004-6361/201423413)
- Bildsten, L., Shen, K. J., Weinberg, N. N., & Nelemans, G. 2007, *The Astrophysical Journal Letters*, 662, L95, doi: [10.1086/519489](https://doi.org/10.1086/519489)
- Brammer, G. B., van Dokkum, P. G., & Coppi, P. 2008, *The Astrophysical Journal*, 686, 1503, doi: [10.1086/591786](https://doi.org/10.1086/591786)
- Brout, D., & Scolnic, D. 2021, *ApJ*, 909, 26, doi: [10.3847/1538-4357/abd69b](https://doi.org/10.3847/1538-4357/abd69b)
- Brout, D., Scolnic, D., Popovic, B., et al. 2022, *The Astrophysical Journal*, 938, 110, doi: [10.3847/1538-4357/ac8e04](https://doi.org/10.3847/1538-4357/ac8e04)
- Bushouse, H., Eisenhamer, J., Dencheva, N., et al. 2022, JWST Calibration Pipeline, Zenodo, doi: [10.5281/zenodo.7325378](https://doi.org/10.5281/zenodo.7325378)
- Casey, C. M., Kartaltepe, J. S., Drakos, N. E., et al. 2023, *The Astrophysical Journal*, 954, 31, doi: [10.3847/1538-4357/acc2bc](https://doi.org/10.3847/1538-4357/acc2bc)
- Chen, W., Kelly, P. L., Frye, B. L., et al. 2024, *ApJ*, 970, 102, doi: [10.3847/1538-4357/ad50a5](https://doi.org/10.3847/1538-4357/ad50a5)
- Childress, M. J., Wolf, C., & Zahid, H. J. 2014, *Monthly Notices of the Royal Astronomical Society*, 445, 1898, doi: [10.1093/mnras/stu1892](https://doi.org/10.1093/mnras/stu1892)
- Coulter, D., Engesser, M., Pierel, J., et al. 2024, *The High-z Menagerie: A Rare Chance to Study the Early and Exotic Transient Universe*
- Coulter, D. A., Pierel, J. D. R., DeCoursey, C., et al. 2025, arXiv e-prints, arXiv:2501.05513, doi: [10.48550/arXiv.2501.05513](https://doi.org/10.48550/arXiv.2501.05513)
- De, K., Kasliwal, M. M., Tzanidakis, A., et al. 2020, *The Astrophysical Journal*, 905, 58, doi: [10.3847/1538-4357/abb45c](https://doi.org/10.3847/1538-4357/abb45c)
- DeCoursey, C., Egami, E., Sun, F., & Jades Collaboration. 2023a, in *American Astronomical Society Meeting Abstracts*, Vol. 55, American Astronomical Society Meeting Abstracts, 206.03
- DeCoursey, C., Egami, E., Rieke, M., et al. 2023b, *Transient Name Server AstroNote*, 164, 1
- DeCoursey, C., Egami, E., Pierel, J. D. R., et al. 2024, arXiv e-prints, arXiv:2406.05060
- DES Collaboration, Abbott, T. M. C., Acevedo, M., et al. 2024, arXiv e-prints, arXiv:2401.02929, doi: [10.48550/arXiv.2401.02929](https://doi.org/10.48550/arXiv.2401.02929)
- Dimitriadis, G., Burgaz, U., Deckers, M., et al. 2024, arXiv e-prints, arXiv:2409.04200, doi: [10.48550/arXiv.2409.04200](https://doi.org/10.48550/arXiv.2409.04200)
- Dunlop, J. S., Abraham, R. G., Ashby, M. L. N., et al. 2021, PRIMER: Public Release IMaging for Extragalactic Research
- Engesser, M., Smith, K., Chen, T., et al. 2022a, *Transient Name Server AstroNote*, 155, 1
- Engesser, M., Brammer, G., Gould, K., et al. 2022b, *Transient Name Server AstroNote*, 145, 1
- Ferruit, P., Jakobsen, P., Giardino, G., et al. 2022, *ÅfÅÿp*, 661, A81, doi: [10.1051/0004-6361/202142673](https://doi.org/10.1051/0004-6361/202142673)
- Filippenko, A. V. 1997, *Annual Review of Astronomy and Astrophysics*, 35, 309, doi: [10.1146/annurev.astro.35.1.309](https://doi.org/10.1146/annurev.astro.35.1.309)
- Fisher, A., Branch, D., Hatano, K., & Baron, E. 1999, *Monthly Notices of the Royal Astronomical Society*, 304, 67, doi: [10.1046/j.1365-8711.1999.02299.x](https://doi.org/10.1046/j.1365-8711.1999.02299.x)
- Fitzpatrick, E. 1999, *Publications of the Astronomical Society of the Pacific*, 111, 63, doi: [10.1086/316293](https://doi.org/10.1086/316293)
- Foley, R. J. 2015, *Monthly Notices of the Royal Astronomical Society*, 452, 2463, doi: [10.1093/mnras/stv789](https://doi.org/10.1093/mnras/stv789)
- Foley, R. J., Hoffmann, S. L., Macri, L. M., et al. 2020, *Monthly Notices of the Royal Astronomical Society*, 491, 5991, doi: [10.1093/mnras/stz3324](https://doi.org/10.1093/mnras/stz3324)
- Foley, R. J., & Mandel, K. 2013, *The Astrophysical Journal*, 778, 167, doi: [10.1088/0004-637X/778/2/167](https://doi.org/10.1088/0004-637X/778/2/167)
- Frye, B. L., Pascale, M., Pierel, J., et al. 2024, *ApJ*, 961, 171, doi: [10.3847/1538-4357/ad1034](https://doi.org/10.3847/1538-4357/ad1034)
- Goldwasser, S., Yaron, O., Sass, A., et al. 2022, *Transient Name Server AstroNote*, 191, 1
- Graham, M. L., Foley, R. J., Zheng, W., et al. 2015, *Monthly Notices of the Royal Astronomical Society*, 446, 2073, doi: [10.1093/mnras/stu2221](https://doi.org/10.1093/mnras/stu2221)
- Grayling, M., Thorp, S., Mandel, K. S., et al. 2024, arXiv e-prints, arXiv:2401.08755, doi: [10.48550/arXiv.2401.08755](https://doi.org/10.48550/arXiv.2401.08755)
- Grogin, N. A., Kocevski, D. D., Faber, S. M., et al. 2011, *ApJS*, 197, 35, doi: [10.1088/0067-0049/197/2/35](https://doi.org/10.1088/0067-0049/197/2/35)
- Guy, J., Astier, P., Baumont, S., et al. 2007, *Astronomy & Astrophysics*, 466, 11, doi: [10.1051/0004-6361:20066930](https://doi.org/10.1051/0004-6361:20066930)
- Horne, K. 1986, *PASP*, 98, 609, doi: [10.1086/131801](https://doi.org/10.1086/131801)
- Hounsell, R., Scolnic, D., Foley, R. J., et al. 2018, *The Astrophysical Journal*, 867, 23, doi: [10.3847/1538-4357/aac08b](https://doi.org/10.3847/1538-4357/aac08b)
- Ivezic, Z., Kahn, S. M., Tyson, J. A., et al. 2019, *The Astrophysical Journal*, 873, 111, doi: [10.3847/1538-4357/ab042c](https://doi.org/10.3847/1538-4357/ab042c)
- Jakobsen, P., Ferruit, P., Alves de Oliveira, C., et al. 2022, *ÅfÅÿp*, 661, A80, doi: [10.1051/0004-6361/202142663](https://doi.org/10.1051/0004-6361/202142663)
- Jönsson, J., Sullivan, M., Hook, I., et al. 2010, *Monthly Notices of the Royal Astronomical Society*, 405, 535, doi: [10.1111/j.1365-2966.2010.16467.x](https://doi.org/10.1111/j.1365-2966.2010.16467.x)
- Kasliwal, M. M., Kulkarni, S. R., Gal-Yam, A., et al. 2012, *The Astrophysical Journal*, 755, 161, doi: [10.1088/0004-637X/755/2/161](https://doi.org/10.1088/0004-637X/755/2/161)
- Kelly, P. L., Hicken, M., Burke, D. L., Mandel, K. S., & Kirshner, R. P. 2010, *The Astrophysical Journal*, 715, 743, doi: [10.1088/0004-637X/715/2/743](https://doi.org/10.1088/0004-637X/715/2/743)
- Kenworthy, W. D., Jones, D. O., Dai, M., et al. 2021, arXiv e-prints, arXiv:2104.07795
- Kessler, R., & Scolnic, D. 2017, *The Astrophysical Journal*, 836, 56, doi: [10.3847/1538-4357/836/1/56](https://doi.org/10.3847/1538-4357/836/1/56)
- Koekemoer, A. M., Aussel, H., Calzetti, D., et al. 2007, *ApJS*, 172, 196, doi: [10.1086/520086](https://doi.org/10.1086/520086)

- Koekemoer, A. M., Faber, S. M., Ferguson, H. C., et al. 2011, *ApJS*, 197, 36, doi: [10.1088/0067-0049/197/2/36](https://doi.org/10.1088/0067-0049/197/2/36)
- Lampeitl, H., Smith, M., Nichol, R. C., et al. 2010, *The Astrophysical Journal*, 722, 566, doi: [10.1088/0004-637X/722/1/566](https://doi.org/10.1088/0004-637X/722/1/566)
- Lu, J., Wang, L., Chen, X., et al. 2022, *The Astrophysical Journal*, 941, 71, doi: [10.3847/1538-4357/ac9f49](https://doi.org/10.3847/1538-4357/ac9f49)
- Mandel, K. S., Thorp, S., Narayan, G., Friedman, A. S., & Avelino, A. 2022, *Monthly Notices of the Royal Astronomical Society*, 510, 3939, doi: [10.1093/mnras/stab3496](https://doi.org/10.1093/mnras/stab3496)
- Mitra, A., Kessler, R., More, S., Hlozek, R., & LSST Dark Energy Science Collaboration. 2023, *ApJ*, 944, 212, doi: [10.3847/1538-4357/acb057](https://doi.org/10.3847/1538-4357/acb057)
- Moreno-Raya, M. E., Mollá, M., López-Sánchez, Á. R., et al. 2016, *The Astrophysical Journal*, 818, L19, doi: [10.3847/2041-8205/818/1/L19](https://doi.org/10.3847/2041-8205/818/1/L19)
- Pascale, M., Frye, B. L., Pierel, J. D. R., et al. 2025, *ApJ*, 979, 13, doi: [10.3847/1538-4357/ad9928](https://doi.org/10.3847/1538-4357/ad9928)
- Perets, H. B., Gal-Yam, A., Mazzali, P. A., et al. 2010, *Nature*, 465, 322, doi: [10.1038/nature09056](https://doi.org/10.1038/nature09056)
- Perlmutter, S., Aldering, G., Goldhaber, G., et al. 1999, *The Astrophysical Journal*, 517, 565, doi: [10.1086/307221](https://doi.org/10.1086/307221)
- Pierel, J. 2024, *Space-Phot: Simple Python-Based Photometry for Space Telescopes*, Zenodo, doi: [10.5281/zenodo.12100100](https://doi.org/10.5281/zenodo.12100100)
- Pierel, J., Engesser, M., Bajaj, V., et al. 2024a, *Do Pass z=2, Do Collect Type Ia Supernovae: Breaking Out of Redshift Jail with JWST*
- Pierel, J. D. R., Rodney, S., Vernardos, G., et al. 2021, *The Astrophysical Journal*, 908, 190, doi: [10.3847/1538-4357/abd8d3](https://doi.org/10.3847/1538-4357/abd8d3)
- Pierel, J. D. R., Jones, D. O., Kenworthy, W. D., et al. 2022, *The Astrophysical Journal*, 939, 11, doi: [10.3847/1538-4357/ac93f9](https://doi.org/10.3847/1538-4357/ac93f9)
- Pierel, J. D. R., Frye, B. L., Pascale, M., et al. 2024b, *The Astrophysical Journal*, 967, 50, doi: [10.3847/1538-4357/ad3c43](https://doi.org/10.3847/1538-4357/ad3c43)
- Pierel, J. D. R., Newman, A. B., Dhawan, S., et al. 2024c, *arXiv e-prints*, arXiv:2404.02139, doi: [10.48550/arXiv.2404.02139](https://doi.org/10.48550/arXiv.2404.02139)
- Pierel, J. D. R., Engesser, M., Coulter, D. A., et al. 2024d, *The Astrophysical Journal Letters*, 971, L32, doi: [10.3847/2041-8213/ad6908](https://doi.org/10.3847/2041-8213/ad6908)
- Rest, A., Pierel, J., Correnti, M., et al. 2023, *arminrest/jhat: The JWST HST Alignment Tool (JHAT)*, Zenodo, doi: [10.5281/zenodo.7892935](https://doi.org/10.5281/zenodo.7892935)
- Rest, A., Stubbs, C., Becker, A. C., et al. 2005, *The Astrophysical Journal*, 634, 1103, doi: [10.1086/497060](https://doi.org/10.1086/497060)
- Riess, A. G., & Livio, M. 2006, *The Astrophysical Journal*, 648, 884, doi: [10.1086/50479110.48550/arXiv.astro-ph/0601319](https://doi.org/10.1086/50479110.48550/arXiv.astro-ph/0601319)
- Riess, A. G., Filippenko, A. V., Challis, P., et al. 1998, *The Astronomical Journal*, 116, 1009, doi: [10.1086/300499](https://doi.org/10.1086/300499)
- Riess, A. G., Yuan, W., Macri, L. M., et al. 2022, *The Astrophysical Journal Letters*, 934, L7, doi: [10.3847/2041-8213/ac5c5b](https://doi.org/10.3847/2041-8213/ac5c5b)
- Rodney, S. A., Riess, A. G., Strolger, L.-G., et al. 2014, *The Astronomical Journal*, 148, 13, doi: [10.1088/0004-6256/148/1/13](https://doi.org/10.1088/0004-6256/148/1/13)
- Rose, B. M., Baltay, C., Hounsell, R., et al. 2021, *arXiv e-prints*, arXiv:2111.03081, doi: [10.48550/arXiv.2111.03081](https://doi.org/10.48550/arXiv.2111.03081)
- Schlafly, E. F., & Finkbeiner, D. P. 2011, *The Astrophysical Journal*, 737, 103, doi: [10.1088/0004-637X/737/2/103](https://doi.org/10.1088/0004-637X/737/2/103)
- Scolnic, D. M., Jones, D. O., Rest, A., et al. 2018, *The Astrophysical Journal*, 859, 101, doi: [10.3847/1538-4357/aab9bb](https://doi.org/10.3847/1538-4357/aab9bb)
- Shen, K. J., Kasen, D., Weinberg, N. N., Bildsten, L., & Scannapieco, E. 2010, *The Astrophysical Journal*, 715, 767, doi: [10.1088/0004-637X/715/2/767](https://doi.org/10.1088/0004-637X/715/2/767)
- Siebert, M. R., Decoursey, C., Coulter, D. A., et al. 2024, *arXiv e-prints*, arXiv:2406.05076
- Sullivan, M., Conley, A., Howell, D. A., et al. 2010, *Monthly Notices of the Royal Astronomical Society*, no, doi: [10.1111/j.1365-2966.2010.16731.x](https://doi.org/10.1111/j.1365-2966.2010.16731.x)
- Tripp, R. 1998, *Astronomy & Astrophysics*, 331, 815
- Waldman, R., Sauer, D., Livne, E., et al. 2011, *The Astrophysical Journal*, 738, 21, doi: [10.1088/0004-637X/738/1/21](https://doi.org/10.1088/0004-637X/738/1/21)
- Ward, S. M., Thorp, S., Mandel, K. S., et al. 2023, *The Astrophysical Journal*, 956, 111, doi: [10.3847/1538-4357/acf7bb](https://doi.org/10.3847/1538-4357/acf7bb)
- Williams, C. C., Oesch, P., Barrufet, L., et al. 2021, *PANORAMIC - A Pure Parallel Wide Area Legacy Imaging Survey at 1-5 Micron*
- Woosley, S. E., Taam, R. E., & Weaver, T. A. 1986, *The Astrophysical Journal*, 301, 601, doi: [10.1086/163926](https://doi.org/10.1086/163926)
- Zenati, Y., Perets, H. B., Dessart, L., et al. 2023, *The Astrophysical Journal*, 944, 22, doi: [10.3847/1538-4357/acaf65](https://doi.org/10.3847/1538-4357/acaf65)